

Quark-Gluon Plasma Fireball

Salah Hamieh, Jean Letessier and Johann Rafelski

Department of Physics, University of Arizona, Tucson, AZ 85721

and Laboratoire de Physique Théorique et Hautes Energies, Université Paris 7, 2 place Jussieu, F-75251 Cedex 05.

(Received: June 17, 2000)

Lattice-QCD results provide an opportunity to model, and extrapolate to finite baryon density, the properties of the quark-gluon plasma (QGP). Upon fixing the scale of the thermal coupling constant and vacuum energy to the lattice data, the properties of resulting QGP equations of state (EoS) are developed. We show that the physical properties of the dense matter fireball formed in heavy ion collision experiments at CERN-SPS are well described by the QGP-EoS we presented. We also estimate the properties of the fireball formed in early stages of nuclear collision, and argue that QGP formation must be expected down to 40A GeV in central Pb-Pb interactions.

PACS: 12.38.Mh, 12.40.Ee, 25.75.-q

I. INTRODUCTION

It is believed today that a new state of matter has been formed in relativistic nuclear collisions at CERN [1]. The existence of a novel non-nuclear high temperature phase of elementary hadron matter, consisting of deconfined quarks and gluons, arises from the current knowledge about quantum chromodynamics (QCD), the theory of strong interaction. At sufficiently high temperature, the strong interactions weaken (asymptotic freedom), and thus we expect that hot and dense nuclear matter will behave akin to a free gas of quarks and gluons [2]. At issue is today if the new phase of matter observed at CERN is indeed this so called quark-gluon plasma (QGP) phase. One of the ways to test, and possibly falsify, the QGP hypothesis is to consider if the expected properties of the QGP indeed agree with experimental data which have been at the center of the CERN announcement.

The observational output of experiments we consider are particle abundances and particle spectra. We address here results on hadron and strange hadron production at the equivalent center of momentum (CM) reaction energy $E_{\text{CM}} = 8.6 \text{ GeV}$ per baryon in Pb-Pb reactions. As seen in many experimental results [1], which we will not restate here in further detail, in these high energy nuclear collisions a localized dense and hot matter fireball is formed. In our earlier analysis of experimental results [3,4], we have obtained diverse physical properties of the source, such as energy per baryon content E/b , entropy per baryon content S/b , and last, not least, strangeness content per baryon \bar{s}/b . These values are associated with temperature T_f and baryo-chemical potential μ_b at which these hadron abundances are produced (chemical freeze out), along with other chemical properties and the collective velocity of the matter emitting these particles v_c .

Our main aim is thus to compare the properties of the QGP phase, modeled to agree with the lattice-QCD calculations [6], to the properties of the fireball obtained in the study of hadronic particle abundances. We thus develop semi-phenomenological QGP equations of state

(EoS) based on thermal and lattice-QCD results. These are then applied to explore, in a systematic fashion, properties of the fireball formed in the Pb-Pb reactions. We show that the physical properties of the fireball extracted from particle production data are the same as obtained employing our QGP-EoS.

Using our QGP-EoS, we also explore the initial thermal conditions reached in the collision both in, and out, of quark chemical equilibrium. We have already shown previously that the strangeness yield is following the predicted QGP yield [3,4]. We also show that, when the energy and baryon number deposited in the initial fireball drops below 20%, *e.g.*, due to large impact parameter interactions, or/and small nuclei involved in the collision, the formation of the QGP phase becomes improbable.

An important dynamical aspect of our experimental data analysis [3,4], on which this work relies, is the sudden disintegration (hadronization) of the fireball into the final state hadrons. This reaction mechanism is a priori not very surprising, since a fireball formed in these collisions explodes, driven by internal compression pressure. However, we did not find in the particle production analysis as the particle source the expected chemically equilibrated, confined hadron phase. Furthermore, the particle production temperature (chemical freeze-out) we found corresponds to a deeply super-cooled state, which can be subject to mechanical instability [7]. We have checked elsewhere this assertion, applying the EoS developed here in a detailed analysis of the fireball sudden break-up, and have found that it occurs at the condition of mechanical instability [8].

A consequence of the sudden fireball break up is that akin to the situation found in the study of properties of the early universe, particle abundances do not reach chemical equilibrium. Our analysis accounts in full for this important fact [3,5]. For an appropriate criticism of the chemical equilibrium models, and a list of related work, we refer the reader to work of Biró [9].

In the next section, we address the thermal QCD interaction coupling α_s we will use. In section III, we define the equations of state and the parameters of our approach

and explore which is the best scheme for the extrapolation of the lattice data. In section IV, we present properties of the QGP phase, relevant both to the study of the freeze-out conditions, and the study of the initial conditions reached in the collision. We present and discuss the comparison of the properties of the exploding fireball with those measured by means of hadron production in section V. Our conclusions follow in section VI.

II. QCD INTERACTIONS IN PLASMA

The energy domain in which we explore diverse properties of dense strongly interacting matter is barely above the scale 1 GeV and thus, in our consideration, an important input is the scale μ dependence of the QCD coupling constant, $\alpha_s(\mu)$, which we obtain solving

$$\mu \frac{\partial \alpha_s}{\partial \mu} = -b_0 \alpha_s^2 - b_1 \alpha_s^3 + \dots \equiv \beta_2^{\text{pert}}. \quad (1)$$

β_2^{pert} is the beta-function of the renormalization group in two loop approximation, and

$$b_0 = \frac{11 - 2n_f/3}{2\pi}, \quad b_1 = \frac{51 - 19n_f/3}{4\pi^2}.$$

β_2^{pert} does not depend on the renormalization scheme, and solutions of Eq. (1) differ from higher order renormalization scheme dependent results by less than the error introduced by the experimental uncertainty in the measured value of $\alpha_s(\mu = M_Z) = 0.118 + 0.001 - 0.0016$. When solving Eq. (1) with this initial condition, we cross several flavor mass thresholds and thus $n_f(\mu)$ is not a constant in the interval $\mu \in (1, 100)$ GeV. Any error made when not properly accounting for n_f dependence on μ accumulates in the solution of Eq. (1). In consequence, a popular approximate analytic solution shown as function of T , as dotted line in figure 1,

$$\alpha_s(\mu) \simeq \frac{2}{b_0 L} \left[1 - \frac{2b_1 \ln \bar{L}}{b_0 L} \right], \quad \bar{L} \equiv \ln(\mu^2/\Lambda^2), \quad (2)$$

with $\Lambda = 0.15$ GeV and $n_f = 3$, is not precise enough compared to the exact 2-loop numerical solution.

We show the numerical solution for $\alpha_s(\mu)$ in figure 1, setting

$$\mu = 2\pi T = \kappa T/T_c, \quad \kappa = 1 \text{ GeV},$$

where the solid line corresponds to $\alpha_s(\mu = M_Z) = 0.118$, bounded by the experimental uncertainty [10]. We observe that $\alpha_s/\pi < 0.25$ is relatively small. However, the expansion parameter of thermal QCD $g = \sqrt{4\pi\alpha_s} > 1$. Therefore even the small difference shown in figure 1 between the approximation (dotted line) used in above references and the exact result is relevant. A large value of g has been a source of considerable concern about validity of perturbative expansion in thermal QCD [11–14].

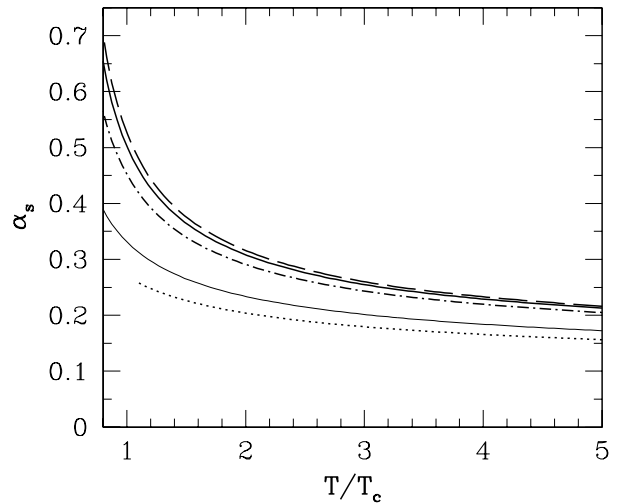


FIG. 1. $\alpha_s(2\pi T)$ for $T_c = 0.16$ GeV. Dashed line: $\alpha_s(M_Z) = 0.119$; solid line = 0.118; dot-dashed line = 0.1156. Dotted line: approximate 2-loop solution given in Eq.(2). Thin solid line: same as dotted, but extrapolating with $n_f = 5$ to $\alpha_s(M_Z) = 0.118$.

The analytical function, Eq. (2), is in fact a very good solution of Eq. (1). For $\Lambda = 0.225$ GeV and $n_f = 5$, it agrees with numerical result for the entire range, $M_Z = 92 \text{ GeV} > \mu > M_B \simeq 4.5 \text{ GeV}$, in which $n_f = \text{Const.}$, here M_B is the bottom quark mass. However, the region of interest for the QGP equations of state we explore is $1 \text{ GeV} < \mu < M_B$, where n_f varies and the approximation, Eq. (2) is not adequate. The thin solid line, in figure 1, shows the behavior of the analytical solution with $n_f = 5$ kept constant, and for $\Lambda = 0.225$ GeV which assures the boundary value $\alpha_s(M_Z) = 0.118$.

III. THE QUARK-GLUON LIQUID

We now can define the quark-gluon liquid model which describes well the properties of QGP determined by lattice-QCD method.

1. To relate the QCD scale to the temperature $T = 1/\beta$, we use for the scale the Matsubara frequency [15]:

$$\mu = 2\pi\beta^{-1} \sqrt{1 + \frac{1}{\pi^2} \ln^2 \lambda_q} = 2\sqrt{(\pi T)^2 + \mu_q^2}. \quad (3)$$

This extension to finite chemical potential μ_q , or equivalently quark fugacity $\lambda_q = \exp \mu_q/T$, is motivated by the form of plasma frequency entering the computation of the vacuum polarization function [16]. In principle, there should be in Eq. (3) also a contribution from the strange quark chemical fugacity λ_s expressed equivalently by the strange quark chemical potential μ_s . However since strangeness conservation virtually assures that $\mu_s \simeq 0$, or equivalently, $\lambda_s \simeq 1$, we will not pursue this further.

2. To reproduce the lattice results available at $\mu_q = 0$

[6], we need to introduce, in the domain of freely mobile quarks and gluons, a finite vacuum energy density:

$$\mathcal{B} = 0.19 \frac{\text{GeV}}{\text{fm}^3}.$$

This also implies, by virtue of relativistic invariance, that there must be a (negative) associated pressure acting on the surface of this volume, aiming to reduce the size of the deconfined region. These two properties of the vacuum follow consistently from the vacuum partition function:

$$\ln \mathcal{Z}_{\text{vac}} \equiv -\mathcal{B}V\beta. \quad (4)$$

3. The partition function of the quark-gluon liquid comprises interacting gluons, n_q flavors of light quarks [17], and the vacuum \mathcal{B} -term. We incorporate further the strange quarks by assuming that their mass in effect reduces their effective number $n_s < 1$:

$$\begin{aligned} \frac{T}{V} \ln \mathcal{Z}_{\text{QGP}} \equiv P_{\text{QGP}} = & -\mathcal{B} + \frac{8}{45\pi^2} c_1 (\pi T)^4 \\ & + \frac{n_q}{15\pi^2} \left[\frac{7}{4} c_2 (\pi T)^4 + \frac{15}{2} c_3 \left(\mu_q^2 (\pi T)^2 + \frac{1}{2} \mu_q^4 \right) \right] \\ & + \frac{n_s}{15\pi^2} \left[\frac{7}{4} c_2 (\pi T)^4 + \frac{15}{2} c_3 \left(\mu_s^2 (\pi T)^2 + \frac{1}{2} \mu_s^4 \right) \right], \quad (5) \end{aligned}$$

where:

$$\begin{aligned} c_1 = 1 - \frac{15\alpha_s}{4\pi} + \dots, \quad (6) \\ c_2 = 1 - \frac{50\alpha_s}{21\pi} + \dots, \quad c_3 = 1 - \frac{2\alpha_s}{\pi} + \dots \end{aligned}$$

In figure 2, the ‘experimental’ values are from numerical lattice simulations of P/T^4 [6]. For practical reasons the lattice results for ‘massless’ 2 and 3-flavors were obtained with $m/T = 0.4$, which reduces the particle numbers by 2%, and this effect is allowed for in the quark-gluon liquid lines (two flavors: dashed, three flavors: dotted) in figure 2. In the case 2+1 flavors, a renormalized strange quark mass $m_s/T = 1.7$, the lattice input has been $m_s^0/T = 1$. This leads to a $\simeq 50\%$ reduction in strange quark number, thus $n_s \simeq 0.5$ will be used in our study of QGP properties, assuming that strangeness is fully chemically equilibrated, unless otherwise noted. Thus, in general, we have $n_f = n_q + n_s \simeq 2.5$.

The thin lines, in figure 2, correspond to the previously reported results for a quark-gluon gas [14], with first order QCD correction introduced using approximate value of $\alpha_s(\mu)$, Eq. (2), without the vacuum pressure term. For $T \geq 2T_c$, the disagreement is an artifact of the approximation for α_s .

Lattice results were also informally reported [1] for the energy density, with $n_f = 3$, and are show in figure 3, upper ‘experimental’ points. The energy density,

$$\epsilon_{\text{QGP}} = -\frac{\partial \ln \mathcal{Z}_{\text{QGP}}(\beta, \lambda)}{V \partial \beta}, \quad (7)$$

is sensitive to the slope of the partition function. We show, in figure 3, the energy density and pressure for two extreme theoretical approaches: the solid lines are for the model we described above ($\mu = 2\pi T$, $\mathcal{B} = 0.19 \text{ GeV}/\text{fm}^3$), the dotted lines are obtained in the thermal expansion, including all, up to fifth order, scale dependent terms obtained by Zhai and Kastening [12], and choosing the scale $\mu = 2.6\pi T$ in free energy and in the coupling constant, so the result reproduces the pressure well (bottom dotted line in figure 3).

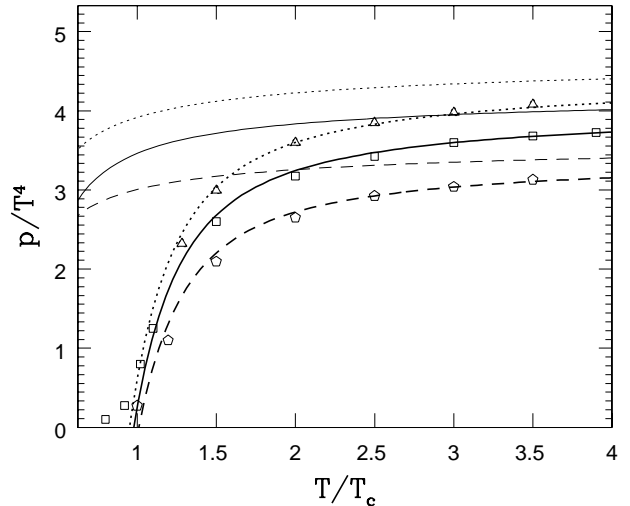


FIG. 2. Lattice-QCD results [6] for P/T^4 at $\lambda_q = 1$, compared with our quark-gluon liquid model (thick lines) and lowest order perturbative QCD using approximate α_s , Eq. (2) (thin lines used in prior work [11–14]); dotted line 3 flavors, solid line 2+1 flavors, and dashed line 2 flavors.

In the upper portion of figure 3, comparing these two theoretical approaches chosen to reproduce the pressure, we see a clear difference in the energy density. The 5th order energy density (dotted line) $(g/4\pi)^5 = (\alpha_s/\pi)^{5/2}/32$ [12], disagrees with the lattice data also at high T , where these are most precise. Near to $T \simeq 1.5T_c$, the solid line is visibly better describing the pressure. In fact, systematic study of the behavior of the $(g/4\pi)^n$ expansion reveals that higher order terms do not lead to a stable result for the range of temperatures of interest to us [12,14].

It is not uncommon to encounter in a perturbative expansion a semi-convergent series. The issue then is how to establish a workable scheme. Our result implies that the choice of the Matsubara frequency $2\pi T$ as the scale μ of the running coupling constant has for yet unknown reasons, the effect to minimize the contribution of the sum of all higher order terms in the expansion Eq. (6), even for moderate temperatures, once the vacuum pressure is introduced. The agreement between our model and the lattice calculations arises despite (or maybe because) the fact that in our evaluation of the temperature dependence of the coupling constant $\alpha_s(T)$ we ignored the dependence of β_2^{pert} on the ambient temperature scale [18]. It seems that in fact the omission of this dependence

conspires with omission of the higher order thermal contributions in the partition function, yielding the remarkable agreement we see between the lattice results and our simple minded approach, which considers the first order corrections in α_s only.

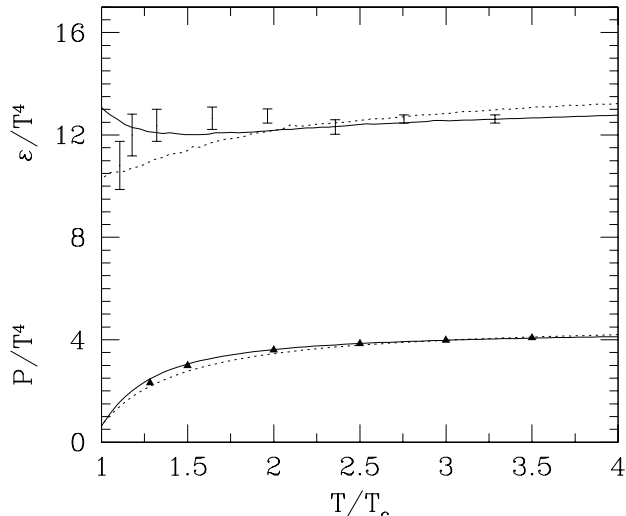


FIG. 3. Top: informal lattice-QCD results [1] for ε/T^4 at $\lambda_q = 1$, compared with our quark-gluon liquid model (solid line). Dotted line is an alternative approach in which all terms in partition function are summed as given in [12] and the scale is set at $\mu = 2.6\pi T$. Bottom: published lattice pressure results [6] compared to the two approaches. Solid line: first order with the bag constant; dotted line: 5th order with $\mu = 2.6\pi T$.

Given that our model adequately describes both pressure and energy density leads us to believe that we also have an appropriate extrapolation scheme for the QGP properties to finite baryon density – but we could not test if the coefficient c_3 , Eq. (6), describes well the behavior of the partition function for finite chemical potentials, as such lattice-QCD results are not available.

In absolute terms, the model we now adopt for further study reproduces the lattice results well, at the level of a few percent. It can only be hoped that the lattice results have reached that level of precision. In our approach, the value of \mathcal{B} we obtain and employ is entirely dependent on the quality of the lattice results. However, in another work [8], we have considered the dynamics of the expanding fireball and obtained an estimate for the value of \mathcal{B} as defined here. We found that $\mathcal{B} \geq 0.17 \text{ GeV}/\text{fm}^3$, consistent with the value we employ here $\mathcal{B} = 0.19 \text{ GeV}/\text{fm}^3$.

IV. PROPERTIES OF QGP-LIQUID

We are now ready to explore the physical properties of the quark-gluon liquid. The energy density is obtained from Eq. (5), recalling that the scale of the interaction is given by Eq. (3):

$$\epsilon_{\text{QGP}} = 4\mathcal{B} + 3P_{\text{QGP}} + A_g + A_q + A_s, \quad (8)$$

$$A_g = (b_0\alpha_s^2 + b_1\alpha_s^3) \frac{2\pi}{3} T^4, \quad (9)$$

$$A_q = (b_0\alpha_s^2 + b_1\alpha_s^3) \left[\frac{5\pi n_q}{18} T^4 + \frac{n_q}{\pi} \left(\mu_q^2 T^2 + \frac{\mu_q^4}{2\pi^2} \right) \right], \quad (10)$$

$$A_s = (b_0\alpha_s^2 + b_1\alpha_s^3) \left[\frac{5\pi n_s}{18} T^4 + \frac{n_s}{\pi} \left(\mu_s^2 T^2 + \frac{\mu_s^4}{2\pi^2} \right) \right]. \quad (11)$$

A convenient way to obtain entropy and baryon density uses the thermodynamic potential \mathcal{F} :

$$\frac{\mathcal{F}(T, \mu_q, V)}{V} = -\frac{T}{V} \ln \mathcal{Z}(\beta, \lambda_q, V)_{\text{QGP}} = -P_{\text{QGP}}. \quad (12)$$

The entropy density is:

$$\begin{aligned} s_{\text{QGP}} &= -\frac{d\mathcal{F}}{V dT}, \quad (13) \\ &= \frac{(n_q + n_s)7\pi^2}{15} c_2 T^3 + n_q c_3 \mu_q^2 T + n_s c_3 \mu_s^2 T \\ &+ \frac{32\pi^2}{45} c_1 T^3 + (A_g + A_q + A_s) \frac{\pi^2 T}{\pi^2 T^2 + \mu_q^2}. \quad (14) \end{aligned}$$

Noting that baryon density is 1/3 of quark density, we have:

$$\begin{aligned} \rho_b &= -\frac{1}{3} \frac{d\mathcal{F}}{V d\mu_q} \quad (15) \\ &= \frac{n_q}{3} c_3 \left\{ \mu_q T^2 + \frac{1}{\pi^2} \mu_q^3 \right\} + \frac{n_s}{3} c_3 \left\{ \mu_s T^2 + \frac{1}{\pi^2} \mu_s^3 \right\} \\ &+ \frac{1}{3} (A_g + A_q + A_s) \frac{\mu_q}{\pi^2 T^2 + \mu_q^2}. \quad (16) \end{aligned}$$

We show properties of the quark-gluon liquid in a wider range of parameters in figure 4. We study the properties at fixed entropy per baryon S/b since an isolated ideal particle fireball would evolve at a fixed S/b . We consider the range $S/b = 10$ (at left for the top panel, baryochemical potential μ_b , and middle panel baryon density n/n_0 , here $n_0 = 0.16/\text{fm}^3$, and bottom left for the energy per baryon E/b) in step of 5 units, up to maximum of $S/b = 60$. The highlighted curve, in figure 4, is for the value $S/b = 42.5$, which value follows from earlier study of hadronic particle spectra [3]. The dotted line, at the minimum of $E/b|_{S/b}$, is where the vacuum and quark-gluon gas pressure balance. This is the equilibrium point and indeed the energy per baryon does have a relative minimum there.

Unlike the case for an ideal quark-gluon gas, the lines of fixed S/b , seen in the top panel of figure 4 are not corresponding to $\mu_b/T = \text{Const.}$, though for large T and small μ_b they do show this asymptotic behavior. Since little entropy is produced during the evolution of the QGP fireball, the thick line in the lower panel of figure 4 describes the approximate trajectory in time of the fireball made in Pb–Pb interactions at the projectile energy 158A GeV. We stress that there has been no adjustment made in any

parameter to bring the earlier determined ‘experimental’ points shown in figure 4 into the remarkable agreement with the properties of equations of state of the quark-gluon plasma, also seen in figure 5.

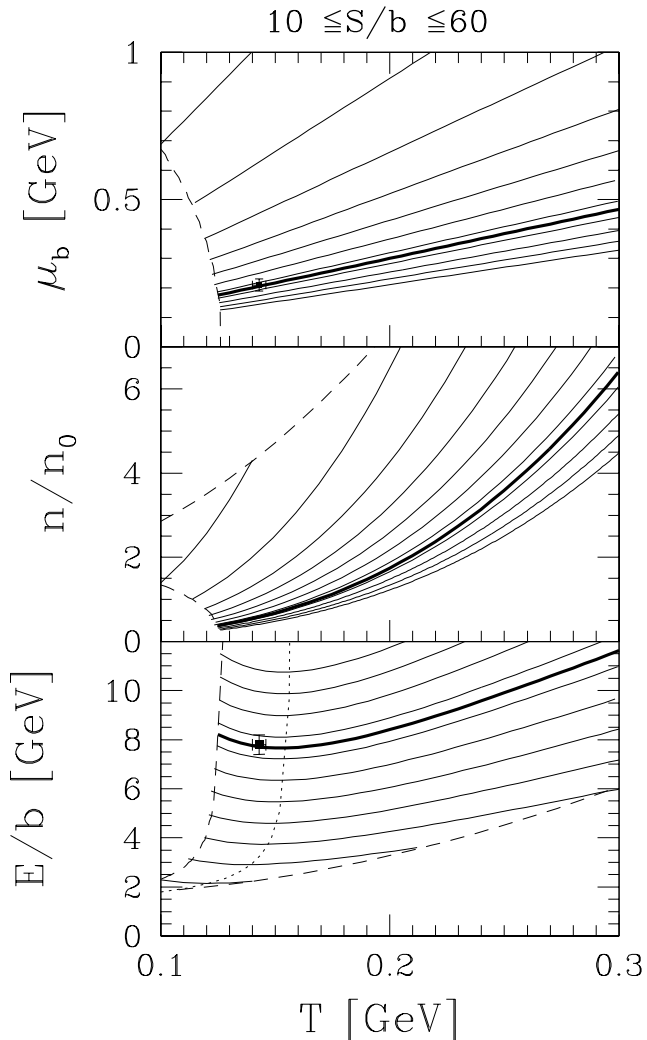


FIG. 4. From top to bottom: μ_b , n/n_0 and E/b ; lines shown correspond to fixed entropy per baryon $S/b = 10$ to 60 by step of 5 (left to right). Thick solid lines: result for $S/b = 42.5$. Limits: energy density $\varepsilon_{q,g} = 0.5 \text{ GeV/fm}^3$ and baryo-chemical potential $\mu_b = 1 \text{ GeV}$. The experimental points denote chemical freeze-out analysis result [3], discussed in section V.

The trajectories at fixed energy per baryon E/b are shown in the T - λ_q plane in figure 5, for the values (beginning at right) $E/b = 2.5$ to 9.5 GeV by step of 1 . The highlighted curve corresponds to the value $E/b = 7.8 \text{ GeV}$ which is the local intrinsic energy content of the hadronizing QGP fireball formed at SPS Pb-Pb interactions at the projectile energy $158A \text{ GeV}$ [3]. Dotted line, in figure 5, corresponds to $P = 0$, the solid line that follows it is the phase transition line where the QGP pressure is balanced by pressure of the hadron gas.

This is the condition at which the equilibrium transition would occur in a slowly evolving system, such as would be the early universe. The properties of hadronic gas are obtained resumming numerically the contribution of all known hadronic particles including resonances, which effectively accounts for the presence of interactions in the confined hadron gas phase [19].

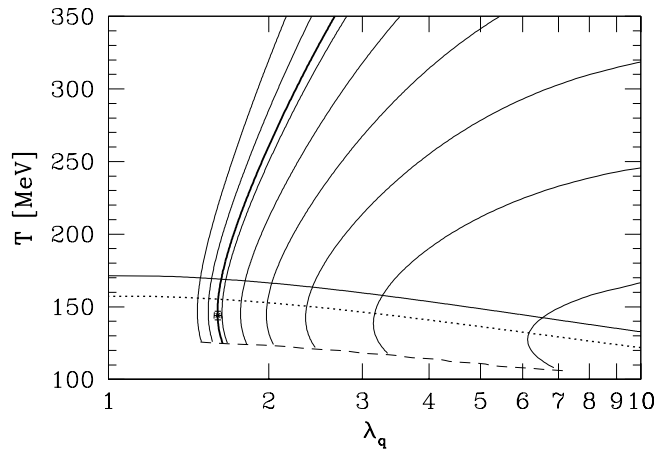


FIG. 5. Contours of constant energy per baryon in QGP in the T - λ_q plane: From right to left $E/b = 2.5$ to 9.5 GeV by step of 1 , thick solid line is for $E/b = 7.8 \text{ GeV}$. Dotted line corresponds to $P = 0$, above this, the solid line is the phase transition where the QGP pressure is balanced by pressure of the hadron gas. The experimental point denotes chemical freeze-out analysis result [3], see section V. Bottom dashed line boundary is at energy density 0.5 GeV/fm^3 .

In relativistic nuclear collisions, the formation of equilibrium state competes with the evolution of the fireball. The slowest of all the equilibria is certainly the chemical equilibration of strange quarks [20]. Next slowest is the equilibration of light quarks. The chemical relaxation time constant for the production of light quarks has been obtained in the first consideration of chemical QGP equilibration, see figure 2 in [20]: $\tau_{GG \rightarrow q\bar{q}}(T = 250 \text{ MeV}) = 0.3 \text{ fm}$. The chemical equilibration of gluons has also been questioned, and is found to be slow, when only $2G \rightarrow 3G$ processes are allowed [21]. Since gluon fusion processes are proportional to the square of gluon abundance, $\tau_{GG \rightarrow q\bar{q}}(T = 250 \text{ MeV}) \rightarrow 1.2 \text{ fm}$ for processes occurring when gluons are at 50% of equilibrium abundance. This explains why quarks trail gluons in the approach to equilibrium, which are struggling to equilibrate by multi-gluon production processes [22]. It is generally assumed that the approximate thermal (kinetic) equilibrium is established much faster. The mechanisms of this process remain under investigation [23].

In figure 6, a case study how the chemical equilibration of quarks cools the gluon-chemically equilibrated fireball is presented. The change of both the initial temperature T_i (upper panel) and λ_q (lower panel) as function of n_f , for $E/b = 9.3 \text{ GeV}$, the total final energy content of Pb-

Pb collisions at CERN, is presented. We see that in the initial state an equilibrated glue phase at $T \simeq 270$ MeV may have been reached. Full chemical equilibrium would correspond to $T \geq 230$ MeV, but more likely this value is somewhat reduced due to flow dilution that has occurred in the process of chemical equilibration.

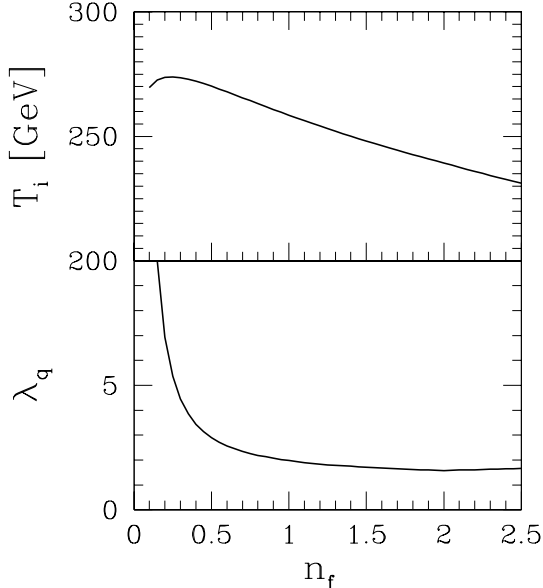


FIG. 6. The initial conditions as function of the number of Fermi degrees of freedom n_f . Upper panel for temperature and lower for quark fugacity, at $E/b = 9.3$ GeV.

One of the interesting quantities is the QGP energy density which we show in figure 7, for both fixed E/b (top) and fixed S/b bottom, for fully equilibrated condition $n_q = 2, n_s = 0.5$. We see that for $E/b > 6$ GeV and $S/b > 25$ the influence of finite baryo-chemical potential is minimal and the lines coalesce. In other words, at conditions we encounter at SPS, we can correlate the energy density with temperature alone $\varepsilon \simeq aT^4$, as seen for $n_f = 3 > 2.5$ in figure 3. In figure 7, we see that the energy density $3 \text{ GeV}/\text{fm}^3$ is established when the temperature in the equilibrated fireball equals 212 MeV. Considering the observed high inverse slopes of strange particles, one can assume that the the plasma phase, before it reached full chemical equilibrium, has been at about $T \simeq 250$ MeV and the energy density in this state has most likely been still higher, above $4 \text{ GeV}/\text{fm}^3$. We believe that our evaluation of the properties of the QGP liquid is, at this range of temperature $T \simeq 1.5T_c$, reliable.

As a final step in the study of the properties of the QGP liquid, we consider the conditions relevant for the formation of the QGP, and consider the behavior for $n_f = 1$. We show, in figure 8, lines of fixed energy per baryon $E/b = 3, 4, 5, 6, 8, 10, 20, 50$ and 100 GeV, akin to results we have shown for $n_f = 2 + 0.5$, in figure 5. The horizontal solid line is where the equilibrated hadronic gas phase has the same pressure as QGP-liquid with semi-equilibrated quark abundance. The free energy of the QGP liquid must be lower (pressure higher) in order for

hadrons to dissolve into the plasma phase. The dotted lines in figure 8, from bottom to top, show where the pressure of the semi-equilibrated QGP phase is equal to $\eta = 20\%, 40\%, 60\%, 80\%$ and 100% , η being the ‘stopping’ fraction of the dynamical collisional pressure [24]:

$$P_{\text{col}} = \eta \rho_0 \frac{P_{\text{CM}}^2}{E_{\text{CM}}}.$$

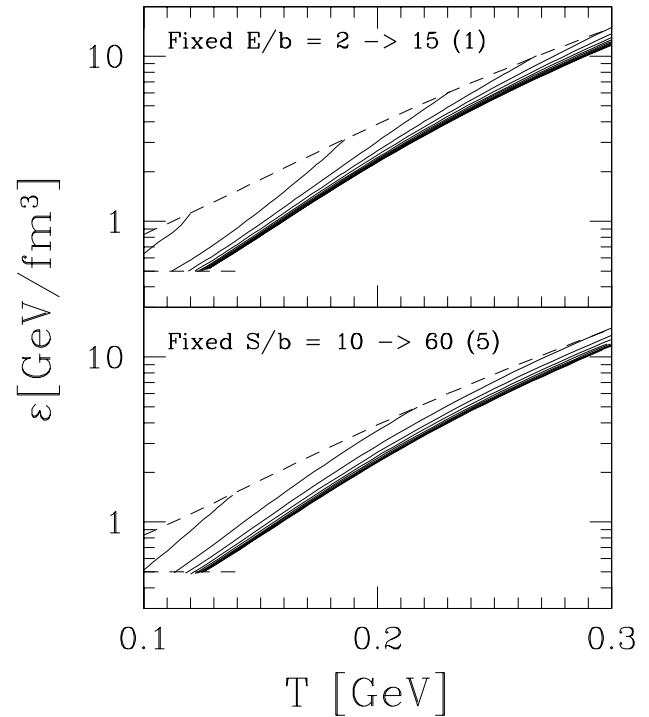


FIG. 7. Energy density in QGP as function of temperature. Top panel: for a fixed Energy per baryon $E/b = 2$ to 15 GeV by step of 1 ; bottom panel for fixed entropy per baryon $S/b = 10$ to 60 by step of 5 . Boundaries are $\varepsilon = 0.5 \text{ GeV}/\text{fm}^3$ at the bottom and $\mu_b = 1 \text{ GeV}$ at the top.

The rationale to study, in figure 8, lines at fixed E/b is that, during the nuclear collision which lasts about $2R_N/\gamma_L 2c \simeq 13/18 \text{ fm}/c$, where γ_L is the Lorentz factor between the lab and CM frame and R_N is the nuclear radius, parton collisions lead to a partial (assumed here to be $1/2$) chemical equilibration of the hadron matter. At that time, the pressure exercised corresponds to collisional pressure P_{col} . This stopping fraction, seen in the transverse energy produced, is about 40% for S–S collisions at $200A$ GeV and 60% for Pb–Pb collisions at $158A$ GeV. If the momentum-energy and baryon number stopping are similar, as we see in the experimental data, then the SPS collisions at 160 – $200A$ GeV are found in the highlighted area left of center of the figure. In the middle of upper boundary of this area, we would expect the beginning evolution of the thermal but not yet chemically equilibrated Pb–Pb fireball, and in the lower left corner of the S–S fireball. We note that the temperature reached

in S–S case is seen to be about 25 MeV lower than in the Pb–Pb case. The lowest dotted line (20% stopping) nearly coincides with the non-equilibrium phase boundary (solid horizontal line, in figure 8) and thus we conclude that this is, for the condition $n_f = 1$, the lowest stopping that can lead to formation of a deconfined QGP phase. Such a low stopping would be encountered possibly in lighter than S–S collision systems or/and at large impact parameter interactions of larger nuclei.

The highlighted area, right of center of the figure 8, corresponds to the expected conditions in Pb–Pb collisions at 40A GeV. If we assume that the stopping here is near 80%, then the initial conditions for fireball evolution would be found towards the upper right corner of this highlighted area. We recognize that the higher stopping nearly completely compensates the effect of reduced available energy in the collision and indeed, we expect that we form QGP also at these collision energies. It is important to realize that we are entering a domain of parameters, in particular λ_q , for which the extrapolation of the lattice results is not necessarily reliable, and thus our equations of state have some systematic uncertainty.

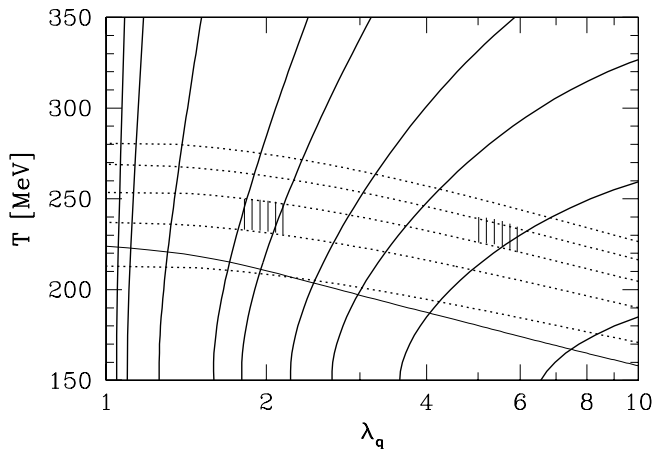


FIG. 8. Contours of energy per baryon in QGP in the T - λ_q plane for $n_f = 1$: From right to left $E/b=3, 4, 5, 6, 8, 10, 20, 50$ and 100 GeV. Thin, nearly horizontal line: hadronic gas phase has the same pressure as the QGP-liquid with semi-equilibrated quark flavor. Dotted lines from bottom to top: pressure in QGP liquid equals 20%, 40%, 60%, 80%, and 100%, of the dynamical collisional pressure.

V. EXPERIMENTAL DATA ANALYSIS AND QGP-EOS

A full account of our prior analysis of the 158A GeV Pb–Pb collision system has appeared [3,4]. We briefly summarize the results that we require for the study of QGP properties at fireball breakup. In table I, in upper section, we present the parameters T_f (the chemical freeze-out temperature), v_c (the collective flow velocity

at sudden breakup), λ_q (the light quark fugacity), λ_s (the strange quark fugacity), γ_q (the light quark phase space occupancy), γ_s (the strange quark phase space occupancy). These are derived from analysis of all hadrons excluding Ω and $\bar{\Omega}$, which data points are not following the same systematic production pattern. These parameters characterize completely the physical properties of the produced hadrons, and these properties are shown in the bottom section of table I.

In the heading of the table, the total error, χ^2 is shown, along with the number of data points N , parameters p and data point constraints r . The confidence level that is reached in our description is near or above 90%, depending on scenario considered. The scenarios we consider are seen in the columns of table I: an unconstrained description of all data in the first column, constraint to exact strangeness conservation in the observed hadrons, second column. Since in both cases the parameter γ_q assumes value that maximizes the entropy and energy content in the pion gas, we assume this value in the so constrained third column.

We can now check the consistency between the statistical parameters (top panel of table I) and the physical properties of the fireball (bottom panel of table I) which are maintained in the process of hadronization. We note that the energy shown in this table, is the intrinsic energy in the flowing frame. The CM-laboratory energy includes the kinetic energy of the flow and thus is greater, to be obtained multiplying the result shown in table I by the Lorentz factor $\gamma = 1/\sqrt{1-v_c^2} = 1.19$. Thus the initial value of the energy per baryon that the system has had before expansion started has been $E^0/b \simeq 9.3$ GeV, as used in figure 6 and in the estimate presented in figure 8.

TABLE I. Results of study of Pb–Pb hadron production [3]: in the heading: the total quadratic relative error χ_{T}^2 , number of data points N , parameters p and redundancies r ; in the upper section: statistical model parameters which best describe the experimental results for Pb–Pb data. Bottom section: specific energy, entropy, anti-strangeness, net strangeness of the full hadron phase characterized by these statistical parameters. In column one, all statistical parameters and the flow vary. In column two, we fix λ_s by requirement of strangeness conservation, and in column three, we fix γ_q at the pion condensation point $\gamma_q = \gamma_q^c$.

	Pb _v	Pb _v ^{sb}	Pb _v ^{sc}
$\chi_{\text{T}}^2; N; p; r$	2.5; 12; 6; 2	3.2; 12; 5; 2	2.6; 12; 5; 2
T_f [MeV]	142 ± 3	144 ± 2	142 ± 2
v_c	0.54 ± 0.04	0.54 ± 0.025	0.54 ± 0.025
λ_q	1.61 ± 0.02	1.605 ± 0.025	1.615 ± 0.025
λ_s	1.09 ± 0.02	1.10*	1.09 ± 0.02
γ_q	1.7 ± 0.5	1.8 ± 0.2	$\gamma_q^{c*} = e^{m_\pi/2T_f}$
γ_s/γ_q	0.79 ± 0.05	0.80 ± 0.05	0.79 ± 0.05
E_f/B	7.8 ± 0.5	7.7 ± 0.5	7.8 ± 0.5
S_f/B	42 ± 3	41 ± 3	43 ± 3
s_f/B	0.69 ± 0.04	0.67 ± 0.05	0.70 ± 0.05
$(\bar{s}_f - s_f)/B$	0.03 ± 0.04	0*	0.04 ± 0.05

In the bottom panel in figure 4, we saw that the Temperature $T_f = 143 \pm 3$ MeV and energy per baryon $E/b = 7.8$ GeV where just at $S/b = 42.5$ seen table I. Similarly, in the top panel, the baryo-chemical potential $\mu_b = 3T_f \ln \lambda_q = 204 \pm 10$ MeV is as required for the consistency of QGP properties. A similarly embarrassing agreement of the hadron yield analysis results with properties of the QGP fireball is seen in figure 5, but that is just a different representation (at fixed E/b) of the result we saw at fixed S/b , in figure 4. However, the importance of this result is that the plasma breakup point appears well below the phase transition temperature line (thin horizontal solid line). As this discussion shows, the properties of the QGP liquid at the point of hadronization are the same as found studying the properties of hadrons emerging from the exploding fireball. Both the specific energy and entropy content of the fireball are consistent with the statistical parameters T_f and μ_b according to our equations of state of the quark-gluon liquid. The freeze-out point at $T \simeq 143$ MeV, seen in bottom panel of figure 4, corresponds to an energy density $\varepsilon_f \simeq 0.6$ GeV/fm³. This is the value for the super-cooled plasma, the equilibrium phase transition occurs at twice this value, $\varepsilon_p \simeq 1.3$ GeV/fm³.

We can also evaluate the hadronic phase space energy density. We need to introduce the excluded volume correction [25]. Considering that the point particle phase space energy density $\varepsilon_{pt} = 1.1$ GeV/fm³, we obtain $\varepsilon_{HG} \simeq 0.4$ GeV/fm³, using the value of $\mathcal{B} = 0.19$ GeV/fm³. Taking into account the numerous uncertainties in the understanding of the excluded volume effect, we conclude that the fireball energy density is comparable in magnitude to the energy density present in hadronic phase space. We also note that the equilibrium phase transition curve we had presented in figure 5 was computed without the excluded volume effect. When allowing for this, the solid line (critical curve) moves about half way towards the dotted line where $P_{QGP} = 0$.

For a vanishing baryo-chemical potential, $\lambda_q = 1$, we determine in figure 5, that the phase transition temperature for point hadrons is $T_p \simeq 172$ MeV. The super-cooled $P = 0$ temperature is at $T_c = 157.5$ MeV (dotted line at $\lambda_q = 1$, in figure 5), and an expanding fireball can super-cool to as low as $T \simeq 145$ MeV, where the mechanical instability occurs [7,8]. We also have seen this result in the bottom panel of figure 4 where the dotted line, corresponding to pressure zero, is to the right of the ‘experimental’ point.

The collective velocity v_c of the exploding matter remains large in deeply super-cooled conditions even though the expansion slows down and kinetic energy is transferred back from flow to thermal component, once the dotted $P = 0$ line is crossed, as can be seen in figure 4. Interestingly, our central value $v_c = 0.54$ is the velocity of sound of the exploding fireball:

$$v_s^2 = \left. \frac{\partial P}{\partial \varepsilon} \right|_{S/b}. \quad (17)$$

The theoretical line shown in figure 9 is computed for $S/b = 42$.

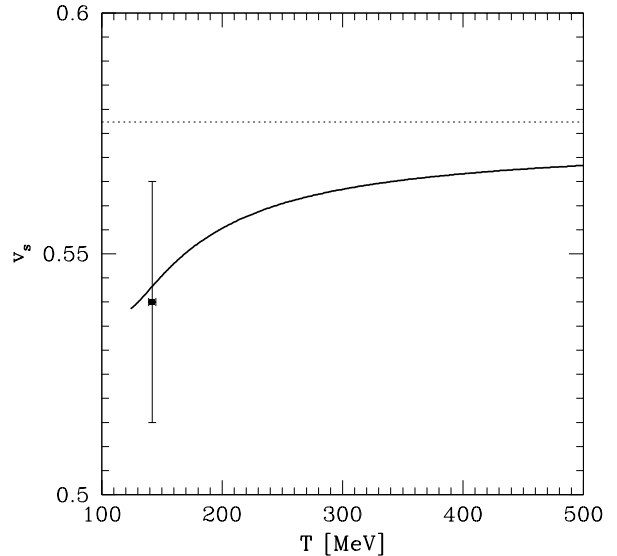


FIG. 9. The velocity of sound of quark-gluon liquid at $S/b = 42$. The dotted line corresponds to the value of the sound velocity of an ideal relativistic gas, $v_s = 1/\sqrt{3}$.

There is yet more evidence for the QGP nature of the fireball. It has been argued before that the values of the three other chemical parameters λ_s, γ_q and γ_s suggest as source a deconfined QGP fireball source [3]:

a) The value of strange quark fugacity λ_s can be obtained from the requirement that strangeness balances, $\langle N_s - N_{\bar{s}} \rangle = 0$, which for a source in which all s and \bar{s} quarks are unbound and thus have symmetric phase space, implies $\lambda_s = 1$. However, the Coulomb distortion of the strange quark phase space plays an important role in the understanding of this constraint for Pb–Pb collisions, leading to the Coulomb-deformed value $\lambda_s \simeq 1.1$, which is identical to the value obtained from experimental data analysis $\lambda_s^a = 1.09 \pm 0.02$.

b) The phase space occupancy of light quarks γ_q is, before gluon fragmentation, near or at the equilibrium value $\gamma_q = 1$. However, as measured by hadron abundances it is expected to significantly exceed unity to accommodate the contribution from gluon fragmentation into light quark pairs. There is an upper limit: $\gamma_q < \gamma_q^c \equiv e^{m_\pi/2T_f} \simeq 1.67$, which arises to maximize the entropy density in the confined hadron phase.

c) The strange quark phase space occupancy γ_s can be computed within the framework of kinetic theory and is mainly influenced by strangeness pair production in gluon fusion [20], in early stages of the collision at high temperature, and by dilution effect in which the already produced strangeness over saturates the ‘thinner’ low temperature phase space. Moreover, some gluon fragmentation also enriches γ_s as measured by hadron abundance. We note that some earlier studies implicitly address the parameter γ_s/γ_q which therefore is stated in table I.

It is worthwhile to recall here that the strangeness yield, $s/b = \bar{s}/b \simeq 0.7$, predicted early on as the result of QGP formation [20] is also one of the results of data analysis seen in table I. This result is found with modern kinetic studies of strangeness production in QGP [3,4,24].

VI. DISCUSSION AND CONCLUSIONS

We have presented properties of the quark-gluon plasma equations of state, and have made several applications pertinent to the physics of relativistic heavy ion collisions. These included a study of the initial attainable conditions reached in Pb–Pb collisions at 158A GeV projectile energy, as well as an evaluation of the hypothesis that direct hadron emission occurs from a disintegrating QGP fireball.

We have based our description of the QCD matter on a form obtained in perturbative expansion of thermal QCD, wherein we have introduced a nonperturbative resummation of the thermal interaction strength. We have also introduced the non-perturbative vacuum properties. The two parameters of our model are the vacuum pressure \mathcal{B} and the scale $\mu(T)$ of the QCD coupling strength. These were chosen to reproduce the latest lattice results for pressure and energy density obtained at zero baryon density. For study of finite baryon density we rely on the perturbative behavior of the interacting quark-gluon gas. This is developed within the same computational approach in which the pressure and energy density are obtained correctly. Fortuitously, it turns out that the QCD interaction effects are smallest for the baryon density, and thus, a priori, are most reliably described. Even so, the magnitude of these effects increases to the level of 45% at the phase boundary.

A serious limitation of our approach is that we rely completely on the current lattice results. There are open questions about the precision of lattice results we model. The requirement for continuum extrapolation [6], and the use of the relatively large $m/T = 0.4$ make our results uncertain at the level of 10%. Moreover, in the deeply supercooled region we do not have lattice results available and the behavior of QGP we consider arises solely from the analytical properties of our QGP model.

In the region of statistical parameters of interest in the discussion of the SPS experimental data, the detail how the baryo-chemical potential enters the interaction scale μ of the strong interaction does not matter since for $(\pi T_c)^2 \simeq 50\mu_q^2$ the μ_b -contribution to the interaction scale is negligible compared to the T -contribution. This, however, means that our successful description of the SPS-experimental results does not imply that our model of QCD matter can safely be used in the study of properties of quark star matter, or the fireball matter made at AGS energies, where $T_c \simeq \mu_q$ [26].

The validity of our equation of state model is better

established in the temperature range pertinent to study of the initial state of the QGP fireball formed at SPS. We have found that during the pre-chemical equilibrium stage of light quarks, the so called hot glue scenario [22], the QGP plasma at SPS has been formed at about $T \simeq 250\text{--}270\text{ MeV}$, see figures 6 and 8. By the time light quarks have also chemically equilibrated, the temperature decreases to just above $T \simeq 210\text{ MeV}$, and the energy density in such a QGP fireball is at $3\text{ GeV}/\text{fm}^3$, as can be seen in the lower panel of figure 7.

We have studied the requirement for the minimal collision energy, which permits the formation of deconfined fireball as function of ‘stopping’ in the collision. We have shown that a significant change in the reaction mechanism of colliding nuclei can be expected when the opacity is at or below 20%, see figure 8. At that point, formation of a deconfined phase fireball is not assured as is seen comparing in the $T\text{--}\lambda_q$ plane the boundary between hadron phase (solid horizontal line in figure 8) and chemically non-equilibrated QGP initial conditions (lowest dashed horizontal line in figure 8). Such a low stopping is expected for sufficiently small collision systems, with participant mass below that seen in central S–S interactions. The results shown in figure 8 imply that the QGP-liquid phase should be formed for Pb–Pb collisions at all collision energies accessible to SPS. In fact, were it not for the uncertainties inherent in the extrapolation of lattice results to high baryon density reached at AGS, we could argue that deconfinement also occurs for Au–Au collisions in the high AGS energy range [27].

We have also compared the properties of the QGP phase to conditions present at time of hadronization, as obtained within an analysis of hadron production [3]. This analysis determines in a first step a set of statistical parameters which describe well experimental hadron multiplicity results. Since this set of parameters also characterizes the phase space of all hadronic particles, in a second step one can estimate the energy, baryon number and entropy content contained in all hadrons produced. A comparison to the QGP equations of state can be made, assuming that in the hadronization of the deconfined matter there has been no reheating, and no shift in chemical equilibrium properties. This is the sudden hadronization. In this case we can compare final state fireball properties with the behavior of QGP matter evaluated at same values of T, λ_q, λ_s .

However, the momentum distribution of final state hadrons could be subject to modification after QGP fireball breakup, which is usually expressed by introducing two sets of statistical parameters, the chemical freeze-out (particle abundance freeze-out) and thermal freeze-out (spectral shape) temperatures and chemical potentials. In our comparison of QGP properties with fireball properties we rely on results obtained from an analysis of particle multiplicity ratios, which reduce the impact of post-hadronization system evolution.

At the time of hadronization of a QGP fireball gluons contribute to form a chemical nonequilibrium excess of

hadrons. Thus even if the hadronizing QGP is (near) chemical equilibrium, the confined phase in general will require allowance for chemical nonequilibrium. A non-equilibrium analysis is more general than the equilibrium models [9], and always describes the hadron production data better [5]. This result in itself constitutes evidence for the presence of primordial deconfined phase. Here, we have for the first time demonstrated that there is a good agreement between the energy, entropy and baryon number content of the collision fireball and the properties expected from the study of supercooled QGP phase.

Although this comparison has produced a very good agreement between the fireball properties and the QGP properties, this could be just a coincidence. Firstly, we do not fully understand the limitations in the description of the fireball matter. The hadron phase space is used with statistical populations allowing for presence of many very heavy hadron resonances. This hypothesis has not been experimentally verified at this time. In fact it is to be expected that a more complex pattern of formation of hadronic particles arises, and we estimate the systematic error in the computed physical properties of hadron phase space to be at least 15%, arising from the assumed populations of unobserved hadronic states. Because of the nature of the QGP equations of state the ‘measurement’ point in figure 4 presented at the values of μ_b and T found from hadron multiplicity analysis would be compatible with a range $35 < S/b < 50$. While it is nice to see the evaluated hadron abundance property to be just it in the middle of this QGP range, we must keep in mind that a wide range of entropy values is permissible.

It must be clearly said that the fireball properties we study are incompatible with properties of chemically and thermally equilibrated confined hadron gas. Perhaps the simplest way to see this is to realize that applying such a model to describe strange hadrons gives a set of parameters which fail to describe the total hadron yield by many (10-15) standard deviations. The key point of our study is that we have shown that a natural way to explain consistently all hadronic production data obtained in 158A GeV Pb–Pb collisions is to invoke as reaction picture the formation, and sequel sudden hadronization, of a QGP fireball.

Acknowledgments

Work supported in part by a grant from the U.S. Department of Energy, DE-FG03-95ER40937. Laboratoire de Physique Théorique et Hautes Energies, LPTHE, at University Paris 6 and 7 is supported by CNRS as Unité Mixte de Recherche, UMR7589.

- [1] <http://www.cern.ch/CERN/Announcements/2000/NewStateMatter>. Text of the scientific consensus view of the spokesmen of CERN experiments also available as: nucl-th/0002042, “Evidence for a New State of Matter: An Assessment of the Results from the CERN Lead Beam Program me”, compilation by U. Heinz and M. Jacob
- [2] J.C. Collins and M.J. Perry, *Phys. Rev. Lett.* **34**, 1353 (1975).
- [3] J. Letessier and J. Rafelski, *Int. J. Mod. Phys. E* **9**, 107 (2000).
- [4] J. Letessier and J. Rafelski, *Acta Phys. Pol. B* **30**, 3559 (1999).
- [5] J. Letessier, and J. Rafelski, *J. Phys. G* **25**, 295 (1998); *Phys. Rev. C* **59**, 947 (1999).
- [6] F. Karsch, E. Laermann and A. Peikert, *Phys. Lett. B* **478**, 447-455, (2000).
- [7] T. Csörgő, and L.P. Csernai, *Phys. Lett. B* **333**, 494 (1994).
- [8] J. Rafelski and J. Letessier “Sudden Hadronization in Relativistic Nuclear Collisions”, hep-ph/0006200, *Phys. Rev. Lett.* in press (2000).
- [9] T.S. Biró, “Quark Coalescence and Hadronic Equilibrium”, hep-ph/0005067.
- [10] J. Letessier, A. Tounsi and J. Rafelski, *Phys. Lett. B* **389**, 586 (1996).
- [11] P. Arnold and C. Zhai, *Phys. Rev. D* **50**, 7603 (1994); **51**, 1906 (1995).
- [12] C. Zhai and B. Kastening, *Phys. Rev. D* **52**, 7232 (1995).
- [13] E. Braaten and A. Nieto, *Phys. Rev. Lett.* **76**, 1417, (1996); and *Phys. Rev. D* **53**, 3421 (1996).
- [14] J. Andersen, E. Braaten and M. Strickland, *Phys. Rev. Lett.* **83**, 2139, (1999); *Phys. Rev. D* **61**, 074016, (2000).
- [15] A. Peshier, B. Kämpfer and G. Soff, *Phys. Rev. C* **61**, 45203, (2000).
- [16] H. Vija and M.H. Thoma, *Phys. Lett. B* **342**, 212, (1995).
- [17] S.A. Chin, *Phys. Lett. B*, **78**, 552, (1978).
- [18] P. Elmfors and R. Kobes, *Phys. Rev. D* **51**, 774 (1995), and references therein.
- [19] R. Hagedorn, *Nuovo Cimento Suppl.* **3**, 147 (1965); Cargèse lectures in Physics, (Gordon and Breach New York 1977) Vol. **6**, and references therein; *Hot Hadronic Matter*, Volume 346 of NATO *Advanced Studies Institute* series B: Physics (Plenum, New York 1995), J. Letessier, H. Gutbrod and J. Rafelski, eds.; H. Grote, R. Hagedorn and J. Ranft, “Atlas of Particle Production Spectra”, CERN black report (December 1970).
- [20] J. Rafelski and B. Müller, *Phys. Rev. Lett.* **48**, 1066 (1982); and **56**, 2334 (1986).
- [21] T. Biró, E. van Doorn, B. Müller, M.H. Thoma and X.-N. Wang, *Phys. Rev., C* **48**, 1275 (1993).
- [22] E. Shuryak, *Phys. Rev. Lett.*, **68**, 3270 (1992); L. Xiong and E.V. Shuryak, *Phys. Rev. C* **49**, 2203 (1994).
- [23] A. Bialas, *Phys. Lett. B* **466**, 301 (1999).
- [24] J. Rafelski, J. Letessier and A. Tounsi, *Acta Phys. Pol. B* **27**, 1035 (1996), and references therein.
- [25] R. Hagedorn and J. Rafelski *Phys. Lett. B* **97**, 136 (1980).
- [26] J. Rafelski and M. Danos, *Phys. Rev. C* **50**, 1684 (1994).
- [27] J. Letessier, J. Rafelski and A. Tounsi, *Phys. Lett. B* **328**, 499 (1994).